

Nesting properties and anisotropy of the Fermi surface of $\text{LuNi}_2\text{B}_2\text{C}$

S.B. Dugdale, M.A. Alam, I. Wilkinson and R.J. Hughes

H.H. Wills Physics Laboratory, University of Bristol, Tyndall Avenue, Bristol BS8 1TL, United Kingdom

I.R. Fisher and P.C. Canfield

Ames Laboratory and Department of Physics and Astronomy, Iowa State University, Ames, Iowa 50011

T. Jarlborg and G. Santi

Département de Physique de la Matière Condensée, Université de Genève, 24 quai Ernest Ansermet, CH-1211 Genève 4, Switzerland

(June 16, 2021)

The rare earth nickel borocarbides, with the generic formula $R\text{Ni}_2\text{B}_2\text{C}$, have recently been shown to display a rich variety of phenomena. Most striking has been the competition between, and even coexistence of, antiferromagnetism and superconductivity. We have measured the Fermi surface (FS) of $\text{LuNi}_2\text{B}_2\text{C}$, and shown that it possesses nesting features capable of explaining some of the phenomena experimentally observed. In particular, it had previously been conjectured that a particular sheet of FS is responsible for the modulated magnetic structures manifest in some of the series. We report the first direct experimental observation of this sheet.

The discovery of superconductivity in the rare earth nickel borocarbides [1] has raised fundamental questions regarding its nature. The presence of moment-bearing rare-earth atoms in addition to high Ni contents makes the very existence of superconductivity surprising, and some of the phenomena associated with its interplay with magnetism have not been observed in any other superconducting material. With the generic formula $R\text{Ni}_2\text{B}_2\text{C}$, some members of the system ($R = \text{Y, Lu, Tm, Er, Ho}$ and Dy), exhibit moderately high values of T_c ($\sim 16\text{K}$, for $R = \text{Y, Lu}$), and are either antiferromagnetic or non-magnetic at low temperature. Two other systems, with $R = \text{Gd, Tb}$, are not superconducting, while the Yb compound shows heavy fermion behavior [2].

One of the most striking observations has been the antiferromagnetic ordering, and its competition (and even coexistence) with superconductivity, conjectured to be driven by a nesting feature in the Fermi surface (FS) [3]. Neutron and x-ray scattering techniques have revealed incommensurate magnetic structures in superconducting Er [4] and Ho [5] compounds, and in the non-superconducting Tb [6] and Gd [7] compounds, characterized by a wave vector $\mathbf{Q}_m \approx (0.55, 0, 0)$. In the Lu compound, the $4f$ band is fully occupied and therefore it is non-magnetic. Since the f electrons occupy localized core-like states, the FS is expected to be similar to that of the other compounds [3]; unfettered by the

complications introduced by the presence of magnetism, the Lu compound is ideal for investigating the origin of the superconductivity in these materials. Where there is magnetic order, the mutual influence of the moments must occur through indirect Ruderman-Kittel-Kasuya-Yosida (RKKY) type interactions; the resulting magnetic structures would then be determined by maxima in the generalized magnetic susceptibility of the conduction electrons. Band theoretical calculations of this susceptibility, $\chi(\mathbf{q})$, in $\text{LuNi}_2\text{B}_2\text{C}$ show a peak around the aforementioned vector, \mathbf{Q}_m , indicating that the magnetic ordering in those other compounds is a result of a common FS nesting feature [3]. Moreover, the presence of strong Kohn anomalies in the phonon dispersion curves of $\text{LuNi}_2\text{B}_2\text{C}$ for wave vectors close to \mathbf{Q}_m has lent additional support to this conjecture [8]. Interest in the FS topology has been enhanced by the observation of a four-fold symmetry in the anisotropy of the upper critical field of $\text{LuNi}_2\text{B}_2\text{C}$ [9]. This has been interpreted in terms of (a) the anisotropy of the underlying FS topology, and (b) the presence of possible three-dimensional d -wave superconductivity [10]. In the absence of any corroborative evidence for the latter suggestion, we shall concentrate on the former. The appearance of the square flux-line lattice (FLL) has been successfully explained through nonlocal corrections to the London theory [11]. In general, there is a nonlocal relationship between the supercurrent, \mathbf{j} , and the vector potential, \mathbf{A} , of the magnetic field in a superconductor, arising from the spatial extent ($\sim \xi_0$) of the Cooper pair [12]. In this scenario, the shape of the FS (which influences the coupling of the supercurrents with the crystal lattice) is responsible for the square FLL observed at high fields in the mixed state and which reverts to the triangular FLL at lower fields [13]. However, despite extensive theoretical work based on the band structures of the non-magnetic Y and Lu compounds [14–16, 3], very few experimental determinations of the electronic structure exist, and many of the predictions, including a “nestable” FS sheet, remain unverified. Most importantly, the de Haas-van Alphen experiments performed on $\text{YNi}_2\text{B}_2\text{C}$ in the superconducting [17] and normal states [18] have not delivered the topo-

logical information necessary to isolate any such features in the FS.

In this Letter, we present a joint experimental and theoretical study of the FS of $\text{LuNi}_2\text{B}_2\text{C}$. The experiment reveals the first direct evidence for the presence of a sheet capable of nesting [3]. Furthermore, we will show that the anisotropy of this FS, as determined by our band structure calculations, is consistent with Kogan's model for the FLL [11].

The occupied momentum states, and hence the FS, can be accessed via the momentum distribution using the 2-Dimensional Angular Correlation of electron-positron Annihilation Radiation (2D-ACAR) technique [19]. A 2D-ACAR measurement yields a 2D projection (integration over one dimension) of an underlying two-photon momentum density,

$$\rho(\mathbf{p}) = \sum_{j,\mathbf{k},\mathbf{G}} n^j(\mathbf{k}) |C_{\mathbf{G},j}(\mathbf{k})|^2 \delta(\mathbf{p} - \mathbf{k} - \mathbf{G}), \quad (1)$$

where $n^j(\mathbf{k})$ is the electron occupation density in \mathbf{k} -space in the j^{th} band, the $C_{\mathbf{G},j}(\mathbf{k})$ are the Fourier coefficients of the interacting electron-positron wave function product and the delta function expresses the conservation of crystal momentum. $\rho(\mathbf{p})$ is a single-centered distribution having the full point symmetry of the crystal lattice in question. In a metal, this distribution contains discontinuities at various points $\mathbf{p}_F = (\mathbf{k}_F + \mathbf{G})$ when a band crosses the Fermi level, E_F . When the FS is of paramount interest, the Lock-Crisp-West procedure [20] is often followed. Here the various FS discontinuities are superimposed by folding $\rho(\mathbf{p})$ (or its measured projections) back into the first Brillouin zone (BZ). The result is a new \mathbf{k} -space density, $\sum_{j,\mathbf{k}} n^j(\mathbf{k}) \sum_{\mathbf{G}} |C_{\mathbf{G},j}(\mathbf{k})|^2$, which aside from the factor $\sum_{\mathbf{G}} |C_{\mathbf{G},j}(\mathbf{k})|^2$ (usually a weak function of \mathbf{k} within each band) is simply the electron occupation density. This well-established technique has recently been used by some of the present authors to identify and measure the FS topology in pure Y [21] and in disordered Gd-Y alloys [22]. The virtue of the 2D-ACAR technique in such studies is that it reveals *directly* the shape of the FS, and hence any propensity for nesting.

The experiments were performed on a single crystal of $\text{LuNi}_2\text{B}_2\text{C}$, grown by a Ni_2B flux method [24]. The sample was cooled to $\sim 50\text{K}$, at which temperature the overall momentum resolution of the Bristol 2D-ACAR spectrometer corresponded to $\sim 10\%$ of the larger BZ dimension. Projections were measured along two different crystallographic directions, a and c . More than 400 million (effective) counts were collected in each spectrum.

The spin-dependent momentum densities were calculated using the linearized muffin-tin orbital (LMTO) method within the atomic sphere approximation (ASA), including combined-correction terms [25]. The exchange-correlation part of the potential was described in the

local density approximation. The self-consistent band-structure was calculated at 594 k -points in the irreducible $1/16^{\text{th}}$ part of the BZ, which to simplify the calculations had the same volume as the standard BZ but a simpler tetragonal shape. We used a basis set of s , p , d and f functions for the Lu, and a reduced (s,p,d) basis set for Ni, B and C. For the calculation of the density-of-states (DOS), and the FS, a denser mesh of 3696 k -points was used. The lattice parameters used were experimental values of $a = 3.464 \text{ \AA}$ and $c = 10.631 \text{ \AA}$ [26]. Electronic wave functions from the dense k -mesh were then used to generate the electron-positron momentum densities, using 1149 reciprocal lattice vectors. A full description of the technique is given in Refs. [25] and [27].

The band-structure obtained (not shown) is very similar to those of Pickett and Singh [16] and Mattheiss [14], and shows that the electronic structure is certainly three-dimensional (compared to the two-dimensional features exhibited in the high- T_c cuprates, e.g. [28]); experimentally, one observes an almost isotropic resistivity [29], which is consistent with this picture. These bands predict a rather complicated FS (shown in Fig. 1), the principal character being Lu d , with some Ni d , and B and C p character [14,16]. The first sheet is a very small electron pocket centered at Γ , while the second is slightly larger and rather more cuboid in shape. It is the third sheet that possesses the nesting properties previously remarked upon [3], but it can also be seen that the second sheet has a square cross section between M and R .

In Figs. 2 and 3, the BZ electron occupancies (both calculated and experimental) are shown, projected along the c and a axes, respectively. The occupied states are indicated by the white areas, and unoccupied by black. The agreement between the positron experiment and the LMTO theory is excellent; one can clearly discern the presence of the Γ -centered electron sheets. The most striking features of Fig. 2 are the electron surfaces with square cross-sections at the corners of the projected BZ. Also noteworthy are the shapes described by the contour lines around this sheet; the protuberances point towards the Γ -point in both the calculation and experiment. Fig. 3 shows fewer features, but demonstrates that the agreement persists when the projection is along a different direction.

Considerable investment has been made in establishing methods of reliably and accurately locating the FS in 2D-ACAR data [30]. Recently, it has been demonstrated that it is possible to accurately caliper the FS from 2D-ACAR data using a criterion based upon edge-detection algorithms employing band-pass filtering or Maximum Entropy techniques [21-23]. In Fig. 4 we present the experimental FS thus derived [21,22], together with a (001) section (passing through the Γ -point) of the calculated third FS sheet. The nesting is indicated by the arrow, and is calipered from the experimental data to be $0.54 \pm 0.02 \times (2\pi/a)$ (our calculation

gives $0.56 \times (2\pi/a)$). Given that the experimental data represent a *projection* of the FS, one does not expect a perfect match between the top and bottom halves of the figure. However, the nesting feature is unequivocally revealed, and its size is in excellent agreement with the pronounced Kohn anomalies close to a wave vector $\mathbf{Q}_m \approx (0.5, 0, 0)$ [8], and the observed incommensurate ordering with $\mathbf{Q}_m \approx (0.55, 0, 0)$ found in the antiferromagnetic compounds. In conjunction with the calculation, it was possible to estimate from the experiment that the fraction of the FS that would be able to participate in nesting is $(4.4 \pm 0.5) \%$, which is consistent with the small increase in the resistivity observed when the current is along [100] [31].

Having shown that the calculated FS topology is in good agreement with our experiment, we derived pertinent quantities from our band structure. The DOS at the Fermi energy, $N(E_F) = 4.3 \text{ (eV cell)}^{-1}$, is similar to values presented by Pickett and Singh [16] and Mattheiss [14] ($4.8 \text{ (eV cell)}^{-1}$). Most importantly, some of the quantities essential to Kogan's theory [11] can be derived from the band structure itself. For the calculation of the Fermi velocities, a special mesh was used, comprising six additional points around each original k -point, to enable accurate evaluation of the relevant derivatives. The Fermi velocities in the ab plane and in the c direction [32] were $\langle v_{F,ab}^2 \rangle^{1/2} = 2.62 \times 10^7 \text{ cm s}^{-1}$, $\langle v_{F,c}^2 \rangle^{1/2} = 2.23 \times 10^7 \text{ cm s}^{-1}$, with masses $m_{ab} = 0.91$, $m_c = 1.26$, implying an average out-of-plane anisotropy in the upper critical field ($(H_{c2}^{<100>} + H_{c2}^{<110>})/2H_{c2}^{<001>}$) of 1.17 compared to an experimental value of 1.16 [9]. A calculation for the isovalent compound $\text{YNi}_2\text{B}_2\text{C}$ predicted 1.02 for this anisotropy, in good agreement with the experimental value of 1.01 [33] and highlighting its sensitivity to the band structure.

In conclusion, we have shown experimentally that the FS topology of $\text{LuNi}_2\text{B}_2\text{C}$ does support nesting, thereby accounting for the anomalies observed in its phonon spectrum [8], and the propensity for magnetic ordering found in some of the other rare-earth nickel borocarbides [2]. In addition, our own calculations of the electronic structure yield a FS in excellent agreement with the experiments, whose anisotropy is consistent with the observation of a square FLL, and with the observed behavior of the upper critical field [9].

The authors would like to thank the EPSRC (UK) for financial support, and B. Harmon and R. Evans for useful discussions. One of us (SBD) acknowledges support from the Lloyd's of London Tercentenary Foundation. Ames Laboratory is operated for the U.S. Department of Energy by Iowa State University under Contract No. W-7405-Eng-82. This work was supported by the Director for Energy Research, Office of Basic Energy Sciences.

- [1] R. Nagarajan *et al.*, Phys. Rev. Lett. **72**, 274 (1994) ; R. J. Cava *et al.*, Nature (London) **367**, 252 (1994).
- [2] P. C. Canfield *et al.*, Physics Today **51**, No.10, 40 (1998).
- [3] J. Y. Rhee, X. Wang and B. N. Harmon, Phys. Rev. B **51**, 15 585 (1995).
- [4] J. Zaretsky *et al.*, Phys. Rev. B **51**, 678 (1995) ; S. K. Sinha *et al.*, Phys. Rev. B **51**, 681 (1995).
- [5] A. I. Goldman *et al.*, Phys. Rev. B **50**, 9668 (1994) ; T. Vogt *et al.*, Phys. Rev. Lett. **75**, 2628 (1995).
- [6] P. Dervenagas *et al.*, Phys. Rev. B **53**, 8506 (1996).
- [7] C. Detlefs *et al.*, Phys. Rev. B **53**, 6355 (1996).
- [8] P. Dervenagas *et al.*, Phys. Rev. B **52**, 9839 (1995) ; H. Kawano *et al.* Phys. Rev. Lett. **77**, 4628 (1996) ; C. Stassis *et al.*, Phys. Rev. B **55** R8678 (1997).
- [9] V. Metlushko *et al.*, Phys. Rev. Lett. **79**, 1738 (1997).
- [10] G. Wang and K. Maki, Phys. Rev. B **58**, 6493 (1998).
- [11] V. G. Kogan *et al.*, Phys. Rev. B **54**, 12 386 (1996) ; V. G. Kogan *et al.*, Phys. Rev. B **55**, R8693 (1997) ; V. G. Kogan *et al.*, Phys. Rev. Lett. **79**, 741 (1997).
- [12] See, e.g., M. Tinkham, *Introduction to Superconductivity* (McGraw-Hill, Singapore, 1996).
- [13] U. Yaron *et al.*, Nature (London) **382**, 236 (1996) ; M. R. Eskildsen *et al.*, Phys. Rev. Lett. **78**, 1968 (1997) ; M. Yethiraj *et al.*, Phys. Rev. Lett. **79**, 4849 (1997) ; Y. DeWilde *et al.*, Phys. Rev. Lett. **78**, 4273 (1997) ; P. L. Gammel *et al.*, Phys. Rev. Lett. **82**, 4082 (1999).
- [14] L. F. Mattheiss, Phys. Rev. B **49**, R13 279 (1994).
- [15] J. I. Lee *et al.*, Phys. Rev. B **50**, 4030 (1994) ; R. Coehoorn, Physica C **228**, 331 (1994) ; H. Kim *et al.*, Phys. Rev. B **52**, 4592 (1995); D. J. Singh, Solid State Commun. **98**, 899 (1996).
- [16] W. E. Pickett and D. J. Singh, Phys. Rev. Lett. **72**, 3702 (1994).
- [17] G. Goll *et al.*, Phys. Rev. B **53**, R8871 (1996).
- [18] L. H. Nguyen *et al.*, J. Low Temp. Phys. **105**, 1653 (1996).
- [19] R. N. West, in *Proceedings of the International School of Physics <<Enrico Fermi>> — Positron Spectroscopy of Solids*, edited by A. Dupasquier and A. P. Mills jr. (IOS Press, Amsterdam, 1995).
- [20] D. G. Lock, V. H. C. Crisp and R. N. West, J. Phys. F **3**, 561 (1973).
- [21] S. B. Dugdale *et al.*, Phys. Rev. Lett. **79**, 941 (1997).
- [22] H. M. Fretwell *et al.*, Phys. Rev. Lett. **82**, 3867 (1999).
- [23] E. A. Livesay *et al.*, J. Phys.:Condens. Matter **11** L279 (1999).
- [24] M. Xu *et al.*, Physica C **227**, 321 (1994).
- [25] O. K. Andersen, Phys. Rev. B **12**, 3060 (1975) ; T. Jarlborg and G. Arbmán, J. Phys. F **7**, 1635 (1977).
- [26] T. Siegrist *et al.*, Nature (London) **357**, 254 (1994).
- [27] A. K. Singh and T. Jarlborg, J. Phys. F **15**, 727 (1985).
- [28] T. Ito *et al.*, Nature (London) **350**, 596 (1991).
- [29] I. R. Fisher *et al.*, Phys. Rev. B **56**, 10820 (1997).
- [30] S. B. Dugdale *et al.*, J. Phys.:Condens. Matter **6**, L435 (1994) ; K. M. O'Brien *et al.*, J. Phys.:Condens. Matter **7**, 925 (1995) ; S. B. Dugdale, Ph.D. thesis, University of Bristol, UK (unpublished) (1996).
- [31] S. L. Bud'ko and P. C. Canfield (unpublished).
- [32] The Fermi velocity averages are as follows : $\langle v^2 \rangle = 1.88 \times 10^{15} \text{ (cm/sec)}^2$, $\langle v_x^4 \rangle = 2.21 \times 10^{30} \text{ (cm/sec)}^4$, $\langle v_x^2 v_y^2 \rangle = 1.63 \times 10^{29} \text{ (cm/sec)}^4$, $\langle v_z^4 \rangle = 6.97 \times 10^{29}$

$$(\text{cm/sec})^4, \langle v_x^2 v_z^2 \rangle = 5.46 \times 10^{29} (\text{cm/sec})^4.$$

[33] E. Johnston-Halperin *et al.*, Phys. Rev. B **51**, 12852 (1995).

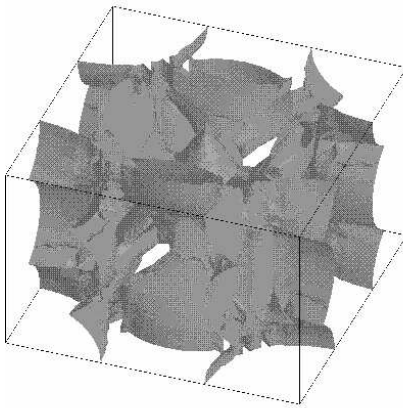
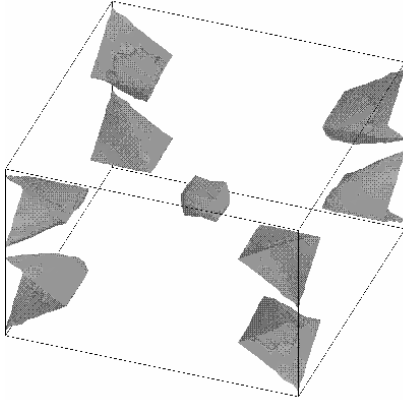
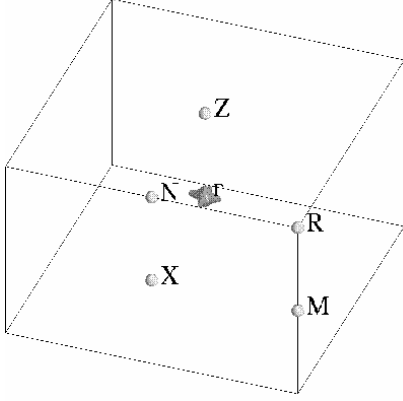


FIG. 1. The three sheets of the FS of $\text{LuNi}_2\text{B}_2\text{C}$, shown within the simple tetragonal BZ (see text), with its usual symmetry points labelled.

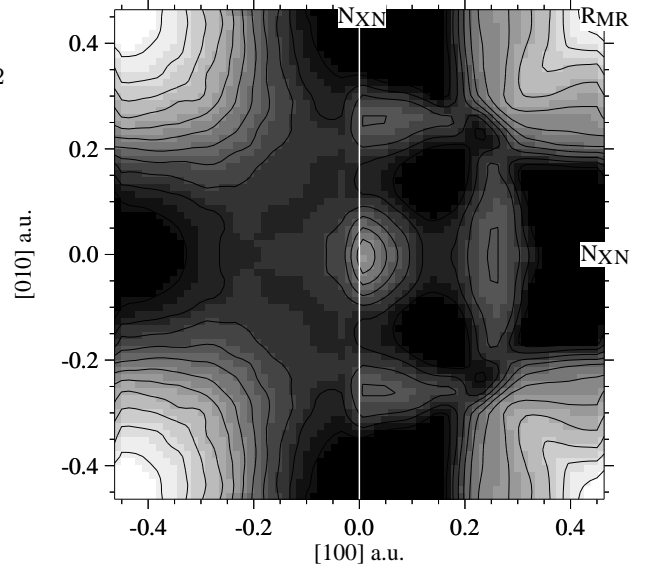


FIG. 2. Experimental (left) and calculated electron density (right) projected along the $[001]$ direction, with the symmetry points of the simple tetragonal BZ indicating the projection path. Black signifies holes, and white represents electrons.

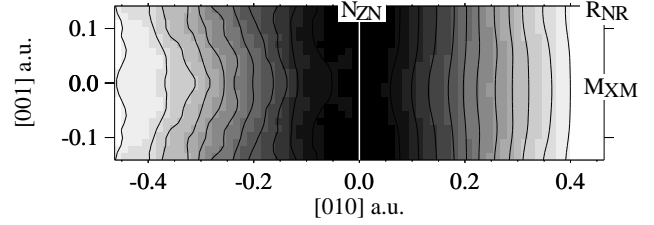


FIG. 3. Experimental (left) and calculated electron density (right) projected along the $[010]$ direction.

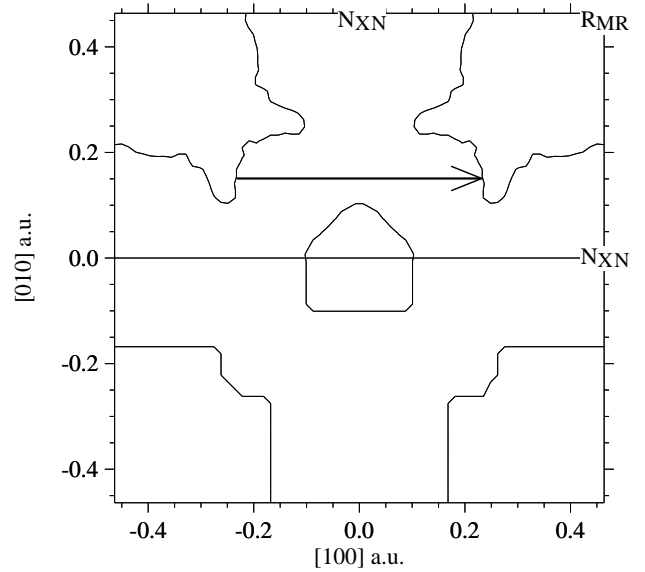


FIG. 4. The experimental (top) and calculated (bottom) FS topology of $\text{LuNi}_2\text{B}_2\text{C}$. The calculation is of the FS in the third band in the (001) plane through the Γ -point. The arrow indicates the nesting feature.